Xylene Recognition in Flexible Porous Coordination Polymer by Guest-Dependent Structural Transition

AUTHOR(S):

Wang, Ping; Kajiwara, Takashi; Otake, Ken-Ichi; Yao, Ming-Shui; Ashitani, Hirotaka; Kubota, Yoshiki; Kitagawa, Susumu

CITATION:

Wang, Ping ...[et al]. Xylene Recognition in Flexible Porous Coordination Polymer by Guest-Dependent Structural Transition. ACS Applied Materials & Interfaces 2021, 13(44): 52144-52151

ISSUE DATE:

2021-11-10

URL:

http://hdl.handle.net/2433/268731

Xylene Recognition in Flexible Porous Coordination Polymer by Guest-dependent Structural Transition

Ping Wang,† Takashi Kajiwara,† Ken-ichi Otake,*,† Ming-Shui Yao,† Hirotaka Ashitani,‡ Yoshiki Kubota,‡ and Susumu Kitagawa*,†

†Institute for Integrated Cell-Material Sciences (WPI-iCeMS), Kyoto University Institute for Advanced Study, Kyoto University, Yoshida Ushinomiya-cho, Sakyo-ku, Kyoto 606-8501, Japan

‡Department of Physical Science, Graduate School of Science, Osaka Prefecture University, 1-1 Gakuen-cho, Naka-ku, Sakai, Osaka 599-8531, Japan

KEYWORDS: xylene separation, porous coordination polymer, metal–organic framework, structural transition, Static separation, breakthrough separation

ABSTRACT: Xylene isomers are crucial chemical intermediates on great demand worldwide; the almost identical physicochemical properties render their current separation approach energy-consuming. In this study, we utilized the soft porous coordination polymer (PCP)'s isomer-specific structural transformation, realizing *o*-xylene (oX) recognition/separation from the binary and ternary isomer mixtures. This PCP has a flexible structure that contains flexible aromatic pendant groups, which both work as recognition sites as well as inducing structural flexibility of the global framework. The PCP exhibits the guest-triggered "breathing"-type structural changes, which are accompanied by the rearrangement of the intraframework π-π interaction. By rebuilding π-π stacking with isomer species, the PCP discriminated oX from the other isomers by specific guest-loading configuration and separated oX from isomer mixture via selective adsorption. The xylene selective property of the PCP is dependent on the solvent; in diluted hexane solution, the PCP favors *p*-xylene (pX) uptake. The separation results combined with crystallographic analyses revealed that the isomer selectivity of the PCP on xylene isomer separation via structural transition and demonstrated its potential as a versatile selective adsorptive medium for challenging separations.

Introduction

Porous coordination polymers (PCPs) are a class of crystalline framework materials built from the coordination bonds of metal clusters and organic ligands.[1-3] Since the discovery of their porous properties, PCPs have been widely investigated as promising adsorptive material.[4-8] Among them, structurally responsive PCP, or flexible PCPs, can often display fascinating structural properties because they have different interconvertible structures depending on external parameters such as temperature, pressure, and guest molecules.[9-16] Flexible PCPs excel conventional porous materials in the recognition ability through the guest-loading-triggered structural transition from the closed to open structures. This phenomenon, often termed as the "gate-opening behavior", can be explained by thermodynamic competition among interactions involving guest molecules and the framework deformation energy. Because of the subtle balance among these energies, the guest recognition in the flexible PCPs can be sensitive enough to discriminate the small difference in the host-guest interaction.[17-24,17-27] By taking advantage of this phenomenon, flexible PCPs have accomplished numerous difficult separation tasks, including CO/N_2,[25,28] O_2/Ar,[26,29] C2 and C3 alkanes [30-33,27-30], and aromatic molecules.[31,34]

Recently, we have developed a new type of flexible PCP (**PCP-1**) which integrates the framework global flexibility and the local flexibility, or the pendant group motion, through the intraframework π-π interaction.[32,35] **PCP-1** contains aromatic pendant groups, which form the multiple intraframework π-π interactions among the aromatic substituents and the framework. The intraframework π-π interactions not only stabilize the porous activated structure but also allow the PCP to have different guest-free forms, depending on the activation approaches, by rearranging the π-π stacking interaction in the framework. Due to its flexible nature, **PCP-1** exhibits the guest-triggered "breathing"-type structural changes, which are accompanied by the rearrangement of the intraframework π-π interaction. Our previous work has demonstrated that the recognition ability of **PCP-1** is sensitive enough to discriminate C6 alkane isomers by isomer-specific gate open pressure. In this work, we expect the aromatic pendant group in the flexible framework of **PCP-1** to work as the mobile and efficient recognition sites for aromatic guest molecules.

Xylene isomer separation is known as a challenging separation task due to their similar physicochemical properties (Supporting Table S1).[33,36] High-purity isomer is in great demand as a valuable chemical intermediate; however, the conventional methods of their separation have been expensive and inefficient processes.[34,37] The preferred way to purify xylene isomers is the adsorptive separation based on the different confinement of the isomers in the nanoscale

pore of the adsorbent.[35, 36, 38, 39] To achieve this, sorting isomer species by using flexible PCPs can be regarded as a promising approach because of the guest responsive gate-opening behavior. In the past decade, several flexible PCPs have been explored for the capability in xylene isomer discrimination.[37-42, 40-46] Typically, these flexible PCPs exhibit a single type of guest accommodated structure; xylene isomers are adsorbed in the almost similar open form of the flexible PCP. In these works, thanks to the difference in preference of the isomers in the pore, the separation of xylene isomers was achieved.

In this study, we explored the capability of **PCP-1** for xylene isomer recognition and separation. Unlike the other flexible PCPs, **PCP-1** can exhibit xylene-isomer-dependent structural change due to the cooperative movement of the PCP framework and aromatic pendant group, which we expect to work as the xylene recognition sites. Xylene isomers have different methyl group positions, which characterize the aryl electron distribution, thus resulting in different π-π stacking preferences. Considering the guest-dependent intraframework π-π stacking, we expect **PCP-1** capable of recognizing and discriminating xylene isomer by forming different types of π-π stacking with amplifying the stacking difference by isomer-specific structural transformation (Figure 1).

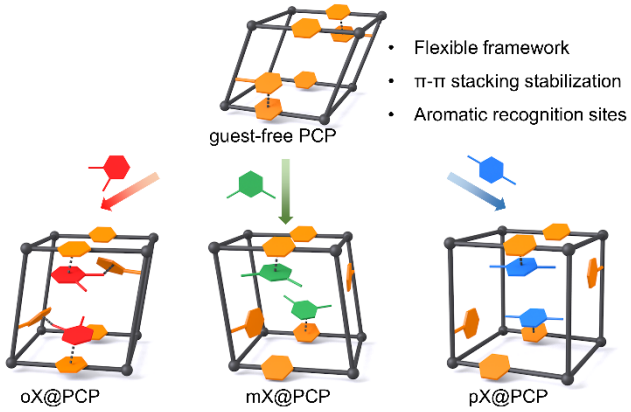

Figure 1. Xylene separation design strategy in flexible **PCP-1. PCP-1** is constructed from the flexible framework (represented as a black lattice) that incorporates intraframework π-π interactions due to the aromatic side chain (represented as yellow hexagons). The aromatic pendant groups play roles as the recognition site for the guest molecules as well as the switch of the PCP structural change.

In the present work, we investigated the xylene isomer recognition capability of **PCP-1** through the combinations of vapor sorption studies, crystallographic X-ray techniques, and liquid phase separation tests. We demonstrated that **PCP-1** exhibits the xylene-isomer-dependent structural changes as revealed from single-crystal structure analysis. In addition, we discovered that **PCP-1** preferred pX adsorption in the closed phase but favored oX uptake when the structural transformation to the open phase occurred. By taking advantage of the flexibility-dependent selectivity, we separated oX from the ternary isomer mixture by both static adsorption and kinetic breakthrough experiment.

Experimental section

PCP synthesis and characterization. The solvothermal synthesis of **PCP-1** was based on a literature procedure.[32-35] Typically, heating a DMF/EtOH mixture solution of $Zn(NO_3)_2{\cdot}6H_2O$, 4,4′-bipyridine (bpy) and the aromatic substituent bearing ligand, 2,5-bis((2-nitrobenzyl)oxy)terephthalic acid (H_2bnta) at 70 ºC for two days gave the single crystal $\{[Zn_2(bnta)_2(bpy)]\cdot(H_2O)_m\ (DMF)_n\}$ (**PCP-1-as**) as yellow bricks. The as-synthesized single crystals were soaked in acetonitrile at room temperature for 24 h for solvent exchange and then heated at 80 °C under dynamic vacuum for 12 h to give fully desolvated PCP powder (**PCP-1-act**).

Liquid-phase batch experiment. For ternary isomer pure mixture adsorption cases, a 4 mL vial with 20 mg **PCP-1-act** was added 1 mL equimolar isomer mixture and kept still 8 h at 298 K. The PCP was then filtered out, washed slightly by hexane, dried in air for 10 min, and analyzed according to weight loss directly by a pyrolyzer-gas chromatography-mass spectrometer (Py-GC-MS). For the adsorption experiment in ternary isomer hexane solution, a 4 mL vial with 20 mg of **PCP-1-act** was added 1 mL equimolar isomer mixture hexane solution and stirred for 8 h at 298 K. The isomer loading PCP was filtered out, slightly washed with hexane and immersed in 1 mL $CDCl_3$ for 2 h. The $CDCl_3$ solution was analyzed by NMR or chromatography-mass spectrometer (GC-MS) to calculate the PCP trapped isomer ratio. For GC-MS, selectivity $\alpha_{i,j}$ was calculated using eq. 1,

$$\alpha_{i,j} = \left(\frac{q_i}{q_j}\right) \times \left(\frac{c_j}{c_i}\right) \qquad \text{(eq. 1)}$$

with q_i and q_j the amounts of isomers i and j adsorbed by **PCP-1-act** and c_j and c_i the equilibrium concentrations of isomers j and i present in the external liquid phase.

For NMR, selectivity $\alpha_{i,j}$ for the equimolar solution was calculated using eq. 2,

$$\alpha_{i,j} = \frac{x_i}{x_j} = \frac{q_i}{q_j} \qquad \text{(eq. 2)}$$

with x_i and x_j the molar fractions of isomers i and j are adsorbed by **PCP-1-act** and q_j and q_i the integrated intensities of isomers i and j methyl groups in the ^{1}H NMR spectra.

Dynamic breakthrough experiments. Approximately 1 g of **PCP-1-act** was dispersed in a vessel with hexane to form a suspension, which was then packed into a stainless-steel column (150 mm length; 4.0 mm i.d.) under 30 MPa using an HPLC pump. A ternary solution of equimolar xylene isomers was pumped over the column at 0.1 mL min^{-1}. The operating pressure reached 10 MPa. Samples at the outlet were collected every 1 min and analyzed by GC. After each experiment, the column was regenerated using a 2 mL min^{-1} solvent flow for 2 h. The column fabrication, breakthrough separation and column regeneration were all conducted at room temperature. The adsorption amount q (mmol) were calculated for each isomer species by integration of the breakthrough curves using eq. 3,

$$q = \int_0^t u(C_{in} - C_{out})dt \qquad \text{(eq. 3)}$$

where u is the volumetric flow rate of the feed (mL min^{-1}), C_{in} and C_{out} are the concentrations of the isomer at the column inlet and out let, respectively (mmol mL^{-1}), and t is the time (min). Selectivity was calculated using *eq.* 1.

Crystal structure analysis. The isomer loaded single crystals were obtained by washing the as-synthesized **PCP-1-as** single-crystal three times using each isomer and immersing the crystal in each isomer for 1 week at 298 K. Single crystals were picked with paraton oil on the tip of glass fiber and mounted on a Rigaku XtaLAB P200 diffractometer equipped with Dectoris PILATUS 200 K detector and Mo−Kα radiation (λ = 0.71073 Å) whose temperature was controlled by liquid nitrogen. Crystal structures were solved by direct methods and refined by full-matrix least-squares cycles in SHELX 2017/1 using Rigaku CrystalStructure ver. 4.3 or Yadokari-XG software package. All non-hydrogen atoms were refined using anisotropic thermal parameters. The refinement results are summarized in Table S2. Crystallographic data for the crystal structures in CIF format has been deposited in the Cambridge Crystallographic Data Centre (CCDC) under deposition numbers CCDC-2081398–2081400. The data can be obtained free of charge via www.ccdc.cam.ac.uk/data_request/cif (or from the Cambridge Crystallographic Data Centre, 12 Union Road, Cambridge CB2 1EZ, U.K.).

Results and discussion

Sample preparation and characterization. We prepared the crystalline sample of the as-synthesized **PCP-1** (**PCP-1-as**) by following the previous literature.[32,35] **PCP-1-as** is composed of the paddlewheel Zn_2 clusters connected with the dicarboxylic acid ligand (H_2bntc), forming two-dimensional (2D) square-grid-like $(Zn_2(bnta)_2)_n$ layers on *ac*-plane, which is further connected to each other by bpy pillar ligand along the *b* axis to form 3D frameworks (Figure S1). Because of the aromatic pendant groups, specifically nitrobenzene substituent on H_2bnta ligand, **PCP-1** forms the π-π stacking interactions among the substituents and the framework itself. We employed the thermal activation method using 80 °C with vacuum drying to obtain the guest-free structure of **PCP-1** (**PCP-1-act**). The complete transformation to **PCP-1-act** was verified by TG and PXRD analyses. Comparing to **PCP-1-as**, the interlayer distance of **PCP-1-act** decreases from 14.0 Å (**PCP-1-as**) to 10.8 Å (**PCP-1-act)**; however, the intraframework π-π interaction between the nitrobenzene-based substituent and the framework was maintained (Figure S1). Because of the aromatic substituent of **PCP-1-act**, we expected **PCP-1-act** could recognize and discriminate the in-pore xylene isomer.

Xylene isomer adsorption at room temperature. To test the xylene-isomers discrimination ability of **PCP-1**, single-component vapor adsorption isotherm measurements at 298 K were firstly conducted (Figure 2a). The adsorption amount of oX soared up from P/P_0 = 0.05, and the uptake almost reaches saturated (31 $cm^3\ g^{-1}$) at P/P_0 = 0.06 and finally stabilized at 44 $cm^3\ g^{-1}$. For mX and pX vapors, the uptake starts late at P/P_0 = 0.07 and slowly moves to the saturated state 40 $cm^3\ g^{-1}$ at P/P_0 = 0.20. Specifically, at P/P_0 = 0.06, the capacity of pX and mX is 6 $cm^3\ g^{-1}$ which is *ca.*20% of the oX uptake at the same pressure. These results of single-component isotherm curves implied that **PCP-1-act** shows a higher affinity toward oX vapor but does not well separate mX and pX vapors. The gate-type sorption behavior indicated that oX vapor triggered the PCP structural transformation quickly at relatively lower pressure (P/P_0 = 0.05) and was adsorbed rapidly. On the other hand, the uptake of mX and pX vapors proceeded sluggishly at larger PCP gate open pressure (P/P_0 = 0.07).

The liquid phase adsorption tests were then studied and characterized by using TGA (Figure 2b) and PXRD (Figure 2c). TGA indicated the xylene loading PCPs were thermal stable until 240°C, which is the same as that of the fresh thermal activated **PCP-1-act** (Figure S2). According to TGA profiles of xylene-isomer adsorbed **PCP-1**, the same weight losses of 14.6 % were observed, which are assignable to trapped xylene (two xylene per the unit cell). This indicated the same amounts of xylene isomers were adsorbed in **PCP-1**. The trapped oX gave off firstly between 67 ℃ to 106 ℃, while pX and mX losing much late between 99 ℃ to 129 ℃. The boiling point of oX (144.4 ℃) is higher than that of mX (139.1 ℃) and pX (138.4 ℃). The inverse weight loss temperature tendency suggested that oX in **PCP-1** might adopt an accommodation fashion different from the other two isomers, which assumption was later confirmed by PXRD of the isomer loaded PCPs. The PXRD pattern of oX loaded PCP (**PCP-1-oX**) differed from those of the two other isomers (**PCP-1-mX** and **PCP-1-pX**) with the additional peaks at 10.7° and 25.1°.

Single-crystal structural analyses of xylene isomer loaded PCP. Inspired by the changes in PXRD patterns depending on guest xylene isomers, we further explored the PCP isomer-specific adsorption by using crystallographic techniques. Fortunately, we could obtain single-crystal structures of the guest-loaded **PCP-1** with all xylene isomers. SXRD reveals that xylene incorporation induced PCP structural transformation, resulting in PCP structures distinct from **PCP-1-act** and **PCP-1-as**. Crystallographically only one type of xylene molecule was detected in each isomer loading PCP. There are two xylene molecules per unit cell, which corresponds to the theoretical vapor adsorption amount of 44 $cm^3\ g^{-1}$ and the TGA weight loss of 14.8%. These calculated values are well consistent with the experimental ones. Interestingly, **PCP-1** exhibits isomer-specific gate-open structures toward xylene isomers due to both the flexible aromatic pendant group and global flexibility of the framework (Figure 3). Firstly, **PCP-1-oX** crystalized in the *P-1* space group with inclined 2D grids (Figure 3a-c). Each pore accommodates two oX molecules per unit cell, which are stabilized by π-π interaction with the terephthalate moiety of the PCP skeleton with a π-π distance of 3.88 Å (Figure 3c). Meanwhile, the nitrobenzyl substituents help to anchor the trapped oX by the multiple interactions between the substituent aryl C-H group and the oX aryl C with C…H distance of 2.73 Å, 2.82 Å and 2.85 Å, respectively (Figure S7). There is an extra interaction from the substituent nitro group (-NO_2) to oX aryl H with an O…H distance of 2.70 Å. As described in the previous literature,[32,35] the stacking between nitrobenzyl substituents and the terephthalate moiety defined **PCP-1-act** configuration. The incorporated oX guest disrupted the π-π stacking between nitrobenzyl substituents and the terephthalate moiety in **PCP-1-act** and replaced aromatic substituents to interact with the framework skeleton, resulting in the PCP oX specific structural transformation. On the other hand, **PCP-1-mX** and **PCP-1-pX** showed the similar configuration of crystal unit cells with the $P4_2/nbc$ space group and channels in perfect square shape (Figure 3d,g). Trapped isomer guests dived in one pore with an aromatic backbone parallel to the crystal unit *c* axis. The isomer molecules partially

overlapped with nitrobenzyl substituents, inducing weak π-π interaction with central arene distance of 4.13 Å in **PCP-1-mX** (Figure 3 e, f) and 4.22 Å in **PCP-1-pX** (Figure 3h, i). In contrast to the weak host-guest interaction, for both mX and pX, robust reciprocity between nitrobenzyl substituents and bpy pillars established by benzene central parts fully overlaying and central distance of 3.72 Å.

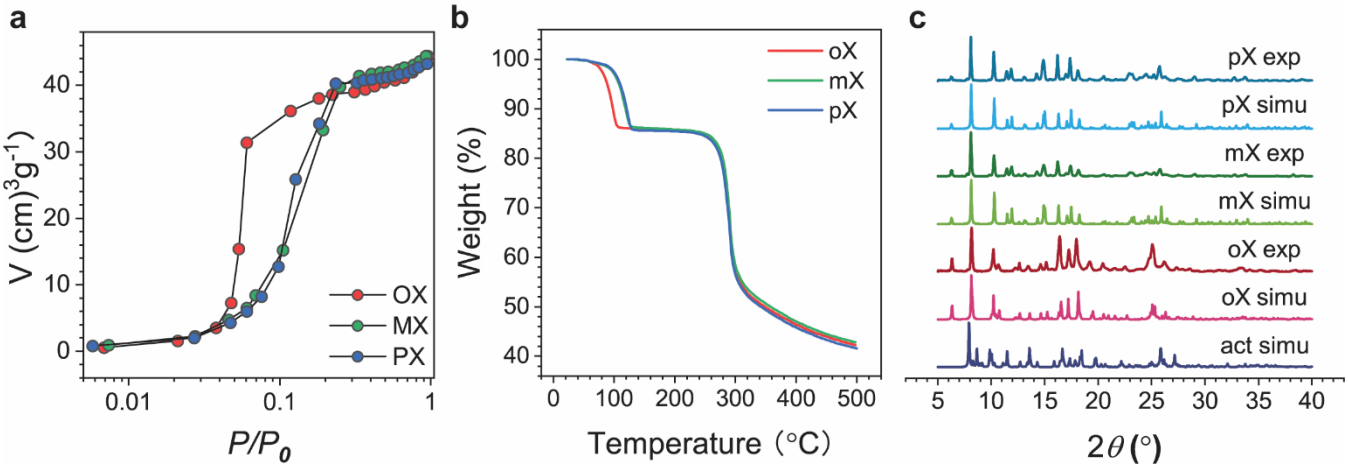

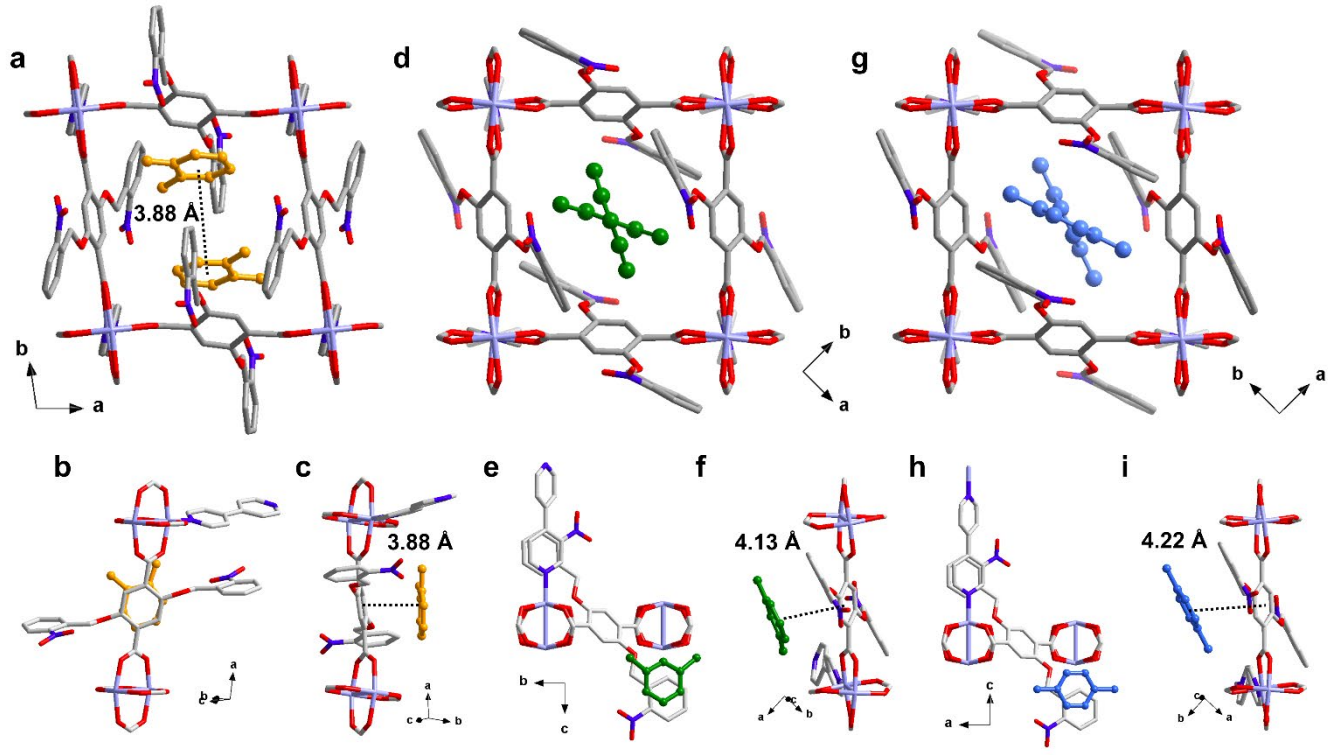

In addition to the π-π attraction from nitrobenzyl substituents, extra host-guest and guest-guest attractions were formed to stabilize the isomer guests. In **PCP-1-mX**, the aligned mX molecules interacted in pairs between the 5-position aryl C-H with a distance of 2.17 Å (Figure S8). Though there is no guest-guest interaction between the aligned pX molecules, in the case of **PCP-1-pX**, host-guest interaction between the substituent methylene C-H and pX aryl C was formed with C...H distance of 2.90 Å (Figure S9). We summarized the observed close contact distances in the crystal structures in Table S3. Apparently, oX formed not only the strongest π-π interaction but also greater numbers of the host-guest/guest-guest interactions are indicated.

The SXRD analysis results clearly showed that oX loaded PCP adopted a configuration distinct from the other two isomer species to facilitate oX molecules π-π staking with framework skeleton. Though all isomer species triggered framework structural transformation, the deformation degree is varied: the deformation degree of **PCP-1-oX** is the smallest. The small deformation degree of **PCP-1-oX** facilitated the framework transformation, thus should be responsible to oX smaller gate open pressure in vapor adsorption experiment.

Static separation. Encouraged by the isomer-specific structural transformation as revealed by SXRD, we explored the separation capability of the PCP via competitive batch experiments. In the experiment, 20 mg of **PCP-1-act** was immersed into a 1 mL binary equimolar mixture. After adsorption, the PCP crystals were filtered out, and the crystal surfaces were slightly washed by hexane and then immersed into 1 mL of NMR solvent ($CDCl_3$) at room temperature to extract the adsorbed xylene isomers. As can be seen from the NMR results, the selective uptake of xylene was completed rapidly within 2 h (Figure S10). The integrated intensities of methyl groups (2.26 ppm for oX, 2.32 ppm for mX and 2.31 ppm for pX) in the ^{1}H NMR spectrum indicated **PCP-1-act** favored oX adsorption with the selectivity oX/mX = 3.4 (Figure 4a) and oX/pX = 3.3. (Figure 4b). Adsorption in equimolar ternary isomer mixture was further explored by Py-GC-MS (Figure S11). The trapped xylene isomers were released upon heating, and the outlet constituent was analyzed directly by GC-MS. As shown in Figure 4c, **PCP-1-act** concentrated oX from the original equimolar mixture by increasing oX content from 33% to 50%. The ratio of trapped mX and trapped pX dropped from 33% to 27% and 23%, respectively. Adsorption selectivity in ternary isomer mixture is oX/pX = 2.2, oX/mX = 1.9 and mX/pX = 1.2. The adsorption process was monitored by Py-GC-MS, confirming the selective uptake completing mostly within 1 h (Figure S12). Therefore, **PCP-1-act** can separate oX from the binary and ternary isomer mixture by selective adsorption, and we attribute the oX favored uptake to the PCP isomer-specific structural transformation. The smallest deformation degree of oX loading configuration facilitates PCP structural transformation in this condition, making oX loading transformation thermodynamically favored.

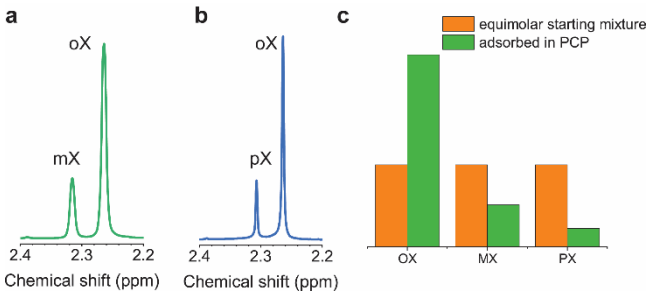

Figure 4. ^{1}H NMR spectra of **PCP-1-act** extracting $CDCl_3$ after binary equimolar mixture adsorption (a) oX and mX and (b) oX and pX. (c) Py-GC-MS result for batch competitive adsorption in equimolar ternary isomer mixture.

Static separation in the diluted condition. We also examined the separation capability of **PCP-1** at the diluted conditions. Batch adsorptive separation experiments were conducted in binary hexane solution of varying concentrations, and the extracted isomer components were analyzed by NMR (Figure 5a, b). As summarized in Table 1, in the concentrated binary solution (isomer concentration ≥ 1M), the PCP preferred oX adsorption as consistent with the result of the pure isomer mixture. However, as opposed to our expectation, in the diluted condition of 0.3 M mixtures, oX adsorption is smaller than the other two isomers with the selectivity of oX/mX = 0.76 and oX/pX = 0.4. Inspired by the interesting reverse selective uptake, we further explored the PCP adsorption in ternary hexane solution, and the selectivity in varied concentration solution was monitored by GC-MS. For ternary solution, in the concentration range from 0.3 M to 2 M, **PCP-1** always adsorbed pX slightly more than the other two isomer species (Figure 5c). In the pure isomer ternary mixture without solvent, the concentration of each isomer equals 2.7 M, and **PCP-1** showed the adsorption capacity toward oX at least two times higher than those toward pX and mX (with the order of oX>mX>pX). While, when diluted by hexane, **PCP-1** selectivity in the ternary mixture inversed with the order of oX<mX<pX (Table 1).

Table 1. Xylene isomer selectivity of PCP-1

C_{isomer}	binary		ternary	
	oX/pX	oX/mX	oX/pX	oX/mX
2.7 M [a]	3.4	3.4	2.2	1.9
2 M [b]	5.5	3.9	0.4	0.6
1 M [b]	4.7	3.0	0.8	1.0
0.3 M [b]	0.4	0.76	1.0	1.2

a, in equimolar pure mixture without solvent and the isomer concentration is 2.7 M.

b, the equimolar isomer mixture was diluted to a certain concentration by hexane.

To investigate the reason for this selectivity inversion, we measured the TGA spectrum of PCP after adsorption in 1 M oX-hexane solution and compared the spectrum with that of pristine oX loaded PCP (Figure S14). The weight loss of solution loading PCP is 3%, which is 1/5 of the pure oX loading sample (14%), indicating that the structure of PCP-1 did not fully convert into the ox-loaded structure in the large presence of hexane. To check the influence of the hexane solvent, we measured the synchrotron PXRD of **PCP-1** immersed in hexane (**PCP-1-hexane**) by sealing activated PCP power and hexane together in a glass capillary. The **PCP-1-hexane** PXRD pattern is not consistent with the **PCP-1-act** simulation pattern and is more similar to that of the open-phase **PCP-1-as** whose pores are occupied by DMF (Figure S15). Therefore, the changes in the xylene-isomer affinity in the existence of hexane might be explained by the solvent competition among the hexane solvent and xylene isomers.

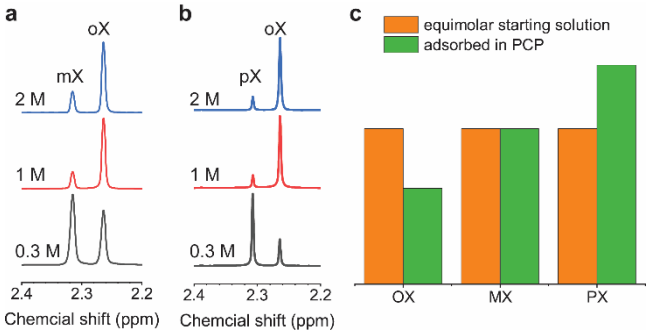

Figure 5. ^{1}H NMR spectra of extracted **PCP-1-act** extracting $CDCl_3$ after binary hexane solution adsorption (a) oX and mX and (b) oX and pX. (c) GC-MS analysis on PCP extracting $CDCl_3$ solution after batch competitive adsorption in 2 M equimolar ternary isomer hexane solution.

Ternary mixture breakthrough experiment. We also conducted the liquid-phase breakthrough experiment using a ternary mixture because of the importance of the separation/recognition capability under flow conditions, as separation processes in industry are typically operated under flow conditions. A constant 0.1 mL min^{-1} flow of a 15 mM ternary isomer hexane solution was pumped over the column (Figure S16). oX appeared in the column outlet after 6 min and during a time interval as long as 10 min, only oX eluted from the column (Figure 6). Next, the breakthrough of mX was observed after an elution time of 16 min. Then, 5 min later, pX appeared from the column outlet at 21 min and flew out at a sluggish rate. After 55 min, the flew-out pX concentration became stable and the same as the inlet value. Therefore, by breakthrough experimental, pure oX component in hexane was obtained from the 15 mM ternary solution in the elution period from 6 min to 16 min. The sequence of flowing out isomers demonstrated that the PCP adsorption preference in the column is pX > mX > oX. The pX selective adsorption is in coincidence with the batch adsorption experiment in hexane solution. The breakthrough separation selectivity of 15 mM ternary mixture solution is estimated as pX/oX=1.8 and pX/mX=1.6, which is better than the selectivity obtained by the static separation using hexane as the solvent (Table 1). The fluid force or the high operating pressure (~10 MPa) applied to the column might also cause some effect on the selective property of **PCP-1** under the dynamic flow condition. When we further increased the isomer concentration to 100 mM, the isomers eluted in the sequence of oX, mX and pX, but the time interval between neighboring species reduced to 1 min, and the overloaded column was no more able to realize their separation (Figure S17). The column can be recycled at least 12 times without obvious decay in the separation performance (Figure S18).

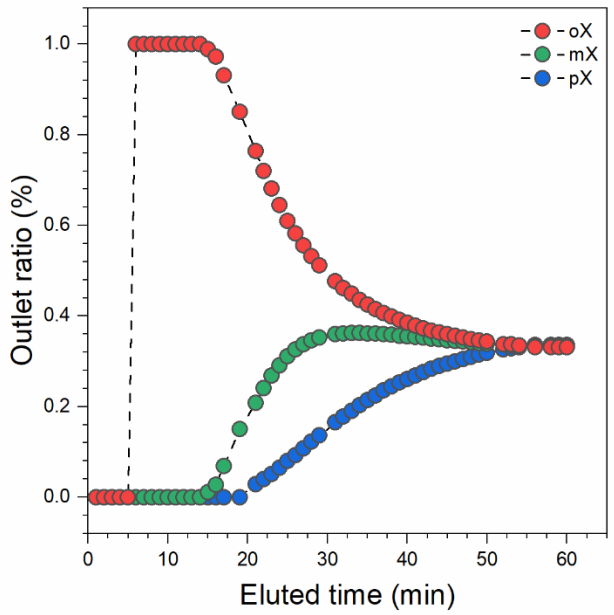

Figure 6. 15 mM breakthrough experiment column using hexane as eluant.

MIL-53 is one of the most well-investigated flexible PCP[37], which xylene-separation mechanisms are thoroughly characterized by various approaches including experimental[42], theoretical calculation[47], and solid-state NMR studies[48]. MIL-53(Al) displayed adsorption selectivity of oX > mX > pX in both static and dynamic separation experiments, and the selectivity did not change in the existence of solvent. Crystallographic analyses showed that the framework structures of xylene-loaded MIL-53(Al) structures were similar to each other. Its oX selectivity was explained by the preferable interactions of methyl groups with the carboxylate moieties in the obtuse pore corners of the 1D channel. Computational modeling[47] and solid-state NMR studies[47,48] also supported the host-guest interaction determined the xylene molecule in-pore diffusion rate, leading to the oX selectivity in dynamic separation experiments. Unlike MIL-53, **PCP-1** exhibits xylene-isomer-dependent structural changes due to the isomer-specific π-π stacking between xylene molecule and PCP skeleton. **PCP-1** exhibited the selectivity of oX > mX > pX from the ternary xylene mixture under the static condition, as following the adsorption preferences. Interestingly, the selective property of **PCP-1** is highly dependent on the condition. The selectivity reversed to pX > mX > oX in the existence of solvent hexane. X-ray studies indicated that the **PCP-1** exhibit the gate-open type structural change upon the adsorption of the solvent hexane. Thus, the changes in the observed affinity might be attributable to an adsorption competition among the solvent and xylene isomers.

Conclusion

In summary, we explored xylene isomer discrimination in a flexibility PCP stabilized by interframework π-π stacking. oX separation from ternary isomer mixture was realized by the PCP isomer-specific structural transformation. The PCP displayed the oX dominant uptake from the equimolar xylene isomer liquid mixture due to the isomer-specific guest-

triggered structural changes (with the affinity of oX>mX>pX). As a result, **PCP-1** enabled concentrating oX from isomer liquid mixture via batch competitive adsorption. On the other hand, when tested under the diluted condition, we observed the inverse isomer selectivity with oX<mX<pX. Therefore, in the dynamic breakthrough experiment using ternary hexane solution, we collected pure oX as the first elute. Our finding demonstrated the specialty of flexible PCPs on challenging isomer recognition/discrimination. With the structural designability as well as the availability of various solvent-dependent flexibility, soft PCPs provide an efficient separate platform for xylene isomer adsorptive separation.

ASSOCIATED CONTENT

The Supporting Information is available free of charge on the ACS Publications website.
X-ray crystallographic data for PCP-1-oX (CIF)
X-ray crystallographic data for PCP-1-mX (CIF)
X-ray crystallographic data for PCP-1-pX (CIF)
Synthetic procedures and characterizations of PCPs, SXRD refinement results, PXRD patterns, TGA, NMR and GC data (PDF)

AUTHOR INFORMATION

*E-mail: ootake.kenichi.8a@kyoto-u.ac.jp
*E-mail: kitagawa@icems.kyoto-u.ac.jp

Author Contributions

All authors have given approval to the final version of the manuscript.

ACKNOWLEDGMENT

This study was supported by KAKENHI Grants-in-Aid for Scientific Research (S) (JP18H05262), Scientific Research (C) (20K05686) and Early-Career Scientists (JP19K15584) from the Japan Society for the Promotion of Science (JSPS). NMR spectroscopy was performed at the iCeMS Analysis Center, Kyoto University Institute for Advanced Study. We thank Nanae Shimanaka at iCeMS, Kyoto University, for her contributions to SXRD analysis.

REFERENCES

(1) Kondo, M.; Yoshitomi, T.; Matsuzaka, H.; Kitagawa, S.; Seki, K. Three-Dimensional Framework with Channeling Cavities for Small Molecules: {[M_2(4, 4′-bpy)$_3$(NO_3)$_4$]·xH_2O}$_n$ (M = Co, Ni, Zn). *Angew. Chem. Int. Ed.* **1997,** *36*, 1725-1727.

(2) Li, H.; Eddaoudi, M.; Groy, T. L.; Yaghi, O. M. Establishing Microporosity in Open Metal–Organic Frameworks: Gas Sorption Isotherms for Zn(BDC) (BDC = 1,4-Benzenedicarboxylate). *J. Am. Chem. Soc.* **1998,** *120*, 8571-8572.

(3) Férey, G.; Serre, C.; Mellot-Draznieks, C.; Millange, F.; Surblé, S.; Dutour, J.; Margiolaki, I. A Hybrid Solid with Giant Pores Prepared by a Combination of Targeted Chemistry, Simulation, and Powder Diffraction. *Angew. Chem. Int. Ed.* **2004,** *43*, 6296-6301.

(4) Li, J.-R.; Kuppler, R. J.; Zhou, H.-C. Selective Gas Adsorption and Separation in Metal–Organic Frameworks. *Chem. Soc. Rev.* **2009,** *38*, 1477-1504.

(5) Adil, K.; Belmabkhout, Y.; Pillai, R. S.; Cadiau, A.; Bhatt, P. M.; Assen, A. H.; Maurin, G.; Eddaoudi, M. Gas/Vapour Separation Using Ultra-Microporous Metal–Organic Frameworks: Insights into the Structure/Separation Relationship. *Chem. Soc. Rev.* **2017,** *46*, 3402-3430.

(6) Kim, J. Y.; Oh, H.; Moon, H. R. Hydrogen Isotope Separation in Confined Nanospaces: Carbons, Zeolites, Metal–Organic Frameworks, and Covalent Organic Frameworks. *Adv. Mater.* **2019**, 31, 1805293.

(7) Barnett, B. R.; Gonzalez, M. I.; Long, J. R. Recent Progress Towards Light Hydrocarbon Separations Using Metal–Organic Frameworks. *Trends in Chemistry* **2019,** *1*, 159-171.

(8) Lin, R.-B.; Xiang, S.; Zhou, W.; Chen, B. Microporous Metal-Organic Framework Materials for Gas Separation. *Chem* **2020,** *6*, 337-363.

(9) Kitagawa, S.; Kitaura, R.; Noro, S. Functional Porous Coordination Polymers. *Angew. Chem. Int. Ed.* **2004,** *43*, 2334-2375.

(10) Horike, S.; Shimomura, S.; Kitagawa, S. Soft Porous Crystals. *Nat. Chem.* **2009,** *1*, 695-704.

(11) Schneemann, A.; Bon, V.; Schwedler, I.; Senkovska, I.; Kaskel, S.; Fischer, R. A. Flexible Metal–Organic Frameworks. *Chem. Soc. Rev.* **2014,** *43*, 6062-6096.

(12) Ze, C.; Dong‐Hui, Y.; Jian, X.; Tong‐Liang, H.; Xian‐He, B. Flexible Metal–Organic Frameworks: Recent Advances and Potential Applications. *Adv. Mater.* **2015,** *27*, 5432-5441.

(13) Bennett, T. D.; Cheetham, A. K.; Fuchs, A. H.; Coudert, F.-X. Interplay Between Defects, Disorder And Flexibility In Metal-Organic Frameworks. *Nat. Chem.* **2017,** *9*, 11-16.

(14) Elsaidi, S. K.; Mohamed, M. H.; Banerjee, D.; Thallapally, P. K. Flexibility in Metal-Organic Frameworks: A Fundamental Understanding. *Coord. Chem. Rev.* **2018,** *358*, 125-152.

(15) Bigdeli, F.; Lollar, C. T.; Morsali, A.; Zhou, H. C. Switching in Metal-Organic Frameworks. *Angew. Chem. Int. Ed.* **2020,** *59*, 4652-4669.

(16) Krause, S.; Hosono, N.; Kitagawa, S. Chemistry of Soft Porous Crystals: Structural Dynamics and Gas Adsorption Properties. *Angew. Chem. Int. Ed.* **2020,** *59*, 15325-15341.

(17) Chen, Q.; Xian, S.; Dong, X.; Liu, Y.; Wang, H.; Olson, D. H.; Williams, L. J.; Han, Y.; Bu, X.-H.; Li, J. High-Efficiency Separation of n-Hexane by a Dynamic Metal-Organic Framework with Reduced Energy Consumption. *Angew. Chem. Int. Ed.* **2021,** *60*, 10593-10597.

(18) Song, B.-Q.; Yang, Q.-Y.; Wang, S.-Q.; Vandichel, M.; Kumar, A.; Crowley, C.; Kumar, N.; Deng, C.-H.; GasconPerez, V.; Lusi, M.; Wu, H.; Zhou, W.; Zaworotko, M. J. Reversible Switching between Nonporous and Porous Phases of a New SIFSIX Coordination Network Induced by a Flexible Linker Ligand. *J. Am. Chem. Soc.* **2020,** *142*, 6896-6901.

(19) Dominik, P. H.; Ryan, A. K.; Michael, A. B.; Benjamin, A. T.; Craig, M. B.; Jeffrey, R. L. Self-Adjusting Binding Pockets Enhance H_2 and CH_4 Adsorption in a Uranium-Based Metal–Organic Framework. *Chem. Sci.* **2020,** *11*, 6709-6716.

(20) Gu, Y.; Zheng, J.-J.; Otake, K.-i.; Sugimoto, K.; Hosono, N.; Sakaki, S.; Li, F.; Kitagawa, S. Structural-Deformation-Energy-Modulation Strategy in a Soft Porous Coordination Polymer with an Interpenetrated Framework. *Angew. Chem. Int. Ed.* **2020,** *59*, 15517 –15521.

(21) Kundu, T.; Wahiduzzaman, M.; Shah, B. B.; Maurin, G.; Zhao, D. Solvent-Induced Control over Breathing Behavior in Flexible Metal-Organic Frameworks for Natural-Gas Delivery. *Angew. Chem. Int. Ed.* **2019,** *58*, 8073-8077.

(22) Suginome, S.; Sato, H.; Hori, A.; Mishima, A.; Harada, Y.; Kusaka, S.; Matsuda, R.; Pirillo, J.; Hijikata, Y.; Aida, T. One-Step Synthesis of an Adaptive Nanographene MOF: Adsorbed Gas-Dependent Geometrical Diversity. *J. Am. Chem. Soc.* **2019,** *141*, 15649-15655.

(23) Kusaka, S.; Kiyose, A.; Sato, H.; Hijikata, Y.; Hori, A.; Ma, Y.; Matsuda, R. Dynamic Topochemical Reaction Tuned by Guest Molecules in the Nanospace of a Metal–Organic Framework. *J. Am. Chem. Soc.* **2019,** *141*, 15742-15746.

(24) Souto, M.; Romero, J.; Calbo, J.; Vitórica-Yrezábal, I. J.; Zafra, J. L.; Casado, J.; Ortí, E.; Walsh, A.; Mínguez Espallargas, G. Breathing-Dependent Redox Activity in a Tetrathiafulvalene-Based Metal–Organic Framework. *J. Am. Chem. Soc.* **2018,** *140*, 10562-10569.

(25) Zhang, X.-W.; Zhou, D.-D.; Zhang, J.-P. Tuning the gating energy barrier of metal-organic framework for molecular sieving. *Chem* **2021**, *7*, 1006-1019.

(26) Gao, Q.; Xu, J.; Cao, D.; Chang, Z.; Bu, X.-H. A Rigid Nested Metal–Organic Framework Featuring a Thermoresponsive Gating Effect Dominated by Counterions. *Angew. Chem. Int. Ed.* **2016**, *55*, 15027-15030.

(27) (3) Yu, M.-H.; Space, B.; Franz, D.; Zhou, W.; He, C.; Li, L.; Krishna, R.; Chang, Z.; Li, W.; Hu, T.-L.; Bu, X.-H. Enhanced Gas Uptake in a Microporous Metal–Organic Framework via a Sorbate Induced-Fit Mechanism. *J. Am. Chem. Soc.* **2019**, *141*, 17703-17712.

(28) Sato, H.; Kosaka, W.; Matsuda, R.; Hori, A.; Hijikata, Y.; Belosludov, R. V.; Sakaki, S.; Takata, M.; Kitagawa, S. Self-Accelerating CO Sorption in a Soft Nanoporous Crystal. *Science* **2014,** *343*, 167-170.

(29) Gu, C.; Hosono, N.; Zheng, J.-J.; Sato, Y.; Kusaka, S.; Sakaki, S.; Kitagawa, S. Design and control of gas diffusion process in a nanoporous soft crystal. *Science* **2019,** *363*, 387-391.

(30) Sen, S.; Hosono, N.; Zheng, J. J.; Kusaka, S.; Matsuda, R.; Sakaki, S.; Kitagawa, S. Cooperative Bond Scission in a Soft Porous Crystal Enables Discriminatory Gate Opening for Ethylene over Ethane. *J. Am. Chem. Soc.* **2017,** *139*, 18313-18321.

(31) Foo, M. L.; Matsuda, R.; Hijikata, Y.; Krishna, R.; Sato, H.; Horike, S.; Hori, A.; Duan, J.; Sato, Y.; Kubota, Y.; Takata, M.; Kitagawa, S. An Adsorbate Discriminatory Gate Effect in a Flexible Porous Coordination Polymer for Selective Adsorption of CO_2 over C_2H_2. *J. Am. Chem. Soc.* **2016,** *138*, 3022-3030.

(32) Wang, X. Q.; Krishna, R.; Li, L. B.; Wang, B.; He, T.; Zhang, Y. Z.; Li, J. R.; Li, J. P. Guest-dependent pressure induced gate-opening effect enables effective separation of propene and propane in a flexible MOF. *Chem. Eng. J.* **2018,** *346*, 489-496.

(33) Li, L. B.; Lin, R. B.; Krishna, R.; Wang, X. Q.; Li, B.; Wu, H.; Li, J. P.; Zhou, W.; Chen, B. L. Flexible-Robust Metal-Organic Framework for Efficient Removal of Propyne from Propylene. *J. Am. Chem. Soc.* **2017,** *139*, 7733-7736.

(34) Zhou, D.-D.; Chen, P.; Wang, C.; Wang, S.-S.; Du, Y.; Yan, H.; Ye, Z.-M.; He, C.-T.; Huang, R.-K.; Mo, Z.-W.; Huang, N.-Y.; Zhang, J.-P. Intermediate-Sized Molecular Sieving of Styrene from Larger and Smaller Analogues. *Nat. Mater.* **2019,** *18*, 994-998.

(35) Wang, P.; Otake, K.-i.; Hosono, N.; Kitagawa, S. Crystal Flexibility Design through Local and Global Motility Cooperation. *Angew. Chem. Int. Ed.* **2021,** *60*, 7030-7035.

(36) Sholl, D. S.; Lively, R. P. Seven Chemical Separations to Change the World. *Nature* **2016,** *532*, 435-437.

(37) Yang, Y.; Bai, P.; Guo, X. Separation of Xylene Isomers: A Review of Recent Advances in Materials. *Ind. Eng. Chem. Res.* **2017,** *56*, 14725-14753.

(38) Li, X.; Wang, J.; Bai, N.; Zhang, X.; Han, X.; da Silva, I.; Morris, C. G.; Xu, S.; Wilary, D. M.; Sun, Y.; Cheng, Y.; Murray, C. A.; Tang, C. C.; Frogley, M. D.; Cinque, G.; Lowe, T.; Zhang, H.; Ramirez-Cuesta, A. J.; Thomas, K. M.; Bolton, L. W.; Yang, S.; Schröder, M. Refinement of Pore Size at Sub-Angstrom Precision in Robust Metal–Organic Frameworks for Separation of Xylenes. *Nat. Commun.* **2020,** *11*, 4280.

(39) Cui, X.; Niu, Z.; Shan, C.; Yang, L.; Hu, J.; Wang, Q.; Lan, P. C.; Li, Y.; Wojtas, L.; Ma, S.; Xing, H. Efficient Separation of Xylene Isomers by a Guest-Responsive Metal–Organic Framework with Rotational Anionic Sites. *Nat. Commun.* **2020,** *11*, 5456.

(40) Warren, J. E.; Perkins, C. G.; Jelfs, K. E.; Boldrin, P.; Chater, P. A.; Miller, G. J.; Manning, T. D.; Briggs, M. E.; Stylianou, K. C.; Claridge, J. B.; Rosseinsky, M. J. Shape Selectivity by Guest-Driven Restructuring of a Porous Material. *Angew. Chem. Int. Ed.* **2014,** *53*, 4592-4596.

(41) Gonzalez, M. I.; Kapelewski, M. T.; Bloch, E. D.; Milner, P. J.; Reed, D. A.; Hudson, M. R.; Mason, J. A.; Barin, G.; Brown, C. M.; Long, J. R. Separation of Xylene Isomers through Multiple Metal Site Interactions in Metal–Organic Frameworks. *J. Am. Chem. Soc.* **2018,** *140*, 3412-3422.

(42) Alaerts, L.; Maes, M.; Giebeler, L.; Jacobs, P. A.; Martens, J. A.; Denayer, J. F. M.; Kirschhock, C. E. A.; De Vos, D. E. Selective Adsorption and Separation of ortho-Substituted Alkylaromatics with the Microporous Aluminum Terephthalate MIL-53. *J. Am. Chem. Soc.* **2008,** *130*, 14170-14178.

(43) Wang, S.-Q.; Mukherjee, S.; Patyk-Kaźmierczak, E.; Darwish, S.; Bajpai, A.; Yang, Q.-Y.; Zaworotko, M. J. Highly Selective, High-Capacity Separation of o-Xylene from C8 Aromatics by a Switching Adsorbent Layered Material. *Angew. Chem. Int. Ed.* **2019,** *58*, 6630-6634.

(44) Shivanna, M.; Otake, K.-i.; Zheng, J.-J.; Sakaki, S.; Kitagawa, S. Control of Local Flexibility towards p-Xylene Sieving in Hofmann-type Porous Coordination Polymers. *Chem. Commun.* **2020,** *56*, 9632-9635.

(45) Sapianik, A. A.; Dudko, E. R.; Kovalenko, K. A.; Barsukova, M. O.; Samsonenko, D. G.; Dybtsev, D. N.; Fedin, V. P. Metal–Organic Frameworks for Highly Selective Separation of Xylene Isomers and Single-Crystal X-ray Study of Aromatic Guest–Host Inclusion Compounds. *ACS Appl. Mater. Interfaces* **2021,** *13*, 14768-14777.

(46) Yang, X.; Zhou, H.-L.; He, C.-T.; Mo, Z.-W.; Ye, J.-W.; Chen, X.-M.; Zhang, J.-P. Flexibility of Metal-Organic Framework Tunable by Crystal Size at the Micrometer to Submillimeter Scale for Efficient Xylene Isomer Separation. *Research* **2019**, *2019*, 9463719.

(47) Rives, S.; Jobic, H.; Kolokolov, D. I.; Gabrienko, A. A.; Stepanov, A. G.; Ke, Y.; Frick, B.; Devic, T.; Férey, G.; Maurin, G. Diffusion of Xylene Isomers in the MIL-47(V) MOF Material: A Synergic Combination of Computational and Experimental Tools. *J. Phys. Chem. C* **2013**, *117*, 6293-6302.

(48) Khudozhitkov, A. E.; Arzumanov, S. S.; Kolokolov, D. I.; Stepanov, A. G. Dynamics of xylene isomers in MIL-53 (Al) MOF probed by solid state 2H NMR. *Microporous Mesoporous Mater.* **2020**, *300*, 110155.

SYNOPSIS TOC (Word Style “SN_Synopsis_TOC”). If you are submitting your paper to a journal that requires a synopsis graphic and/or synopsis paragraph, see the Instructions for Authors on the journal’s homepage for a description of what needs to be provided and for the size requirements of the artwork.